Biomaterials 29 (2008) 4471–4480

Contents lists available at ScienceDirect

Biomaterials

journal homepage: www.elsevier.com/locate/biomaterials

Leading Opinion

Embryoid body morphology influences diffusive transport of inductive biochemicals: A strategy for stem cell differentiation☆

Eleftherios Sachlos, Debra T. Auguste*

School of Engineering and Applied Sciences, Harvard University, 29 Oxford Street, Cambridge, MA 02138, USA

ARTICLE INFO

Article history:
Received 10 July 2008
Accepted 20 August 2008
Available online 14 September 2008

Keywords:
Human embryonic stem cells
Embryoid bodies
Diffusion
Differentiation
Collagen
Extracellular matrix

ABSTRACT

Differentiation of human embryonic stem (hES) cells into cells for regenerative medicine is often initiated by embryoid body (EB) formation. EBs may be treated with soluble biochemicals such as cytokines, growth factors and vitamins to induce differentiation. A scanning electron microscopy analysis, conducted over 14 days, revealed time-dependent changes in EB structure which led to the formation of a shell that significantly reduced the diffusive transport of a model molecule (374 Da) by >80%. We found that the shell consists of 1) an extracellular matrix (ECM) comprised of collagen type I; 2) a squamous cellular layer with tight cell–cell adhesions associated with E-cadherin; and 3) a collagen type IV lining indicative of a basement membrane. Disruption of the basement membrane, by either inhibiting its formation with noggin or permeabilizing it with collagenase, resulted in recovery of diffusive transport. Increasing the diffusive transport of retinoic acid (RA) and serum in EBs by a 15-min collagenase digestion on days 4, 5, 6 and 7 promoted neuronal differentiation. Flow cytometry and quantitative RT-PCR analysis of collagenase-treated EBs revealed 68% of cells expressing neural cell adhesion molecule (NCAM) relative to 28% for untreated EBs. Our results suggest that limitations in diffusive transport of biochemicals need to be considered when formulating EB differentiation strategies.

1. Introduction

EBs recapitulate the early stages of embryonic development and therefore provide a unique system for differentiation of human embryonic stem cells. EBs begin as suspended hES cell aggregates which transform into three-dimensional cystic bodies that comprise the three germ lineages. Exogenous soluble biochemicals such as retinoic acid [1–3], ascorbic acid [4,5], dimethyl sulfoxide [6,7], interleukins [8,9], bone morphogenetic proteins (BMPs) [8,10,11] basic fibroblastic growth factor (bFGF) [12] and activin A (activin) [13] are frequently used to stimulate EBs to differentiate towards a specific lineage. These exogenous biochemicals are added as supplements to the media. Complicated protocols involving variations in duration of biochemical exposure, concentration of biochemicals, time points for EB dissociation and multiple stages of exposure to various biochemicals have been reported [2,8,9,11,12]. Using these strategies, embryonic stem cells have been differentiated into several cell types, including neurons [1], cardiomyocytes [6], hematopoietic cells [8,14], adipocytes [7] and chondrocytes [10]. The inductive potential of soluble biochemicals is therefore dependent on their diffusive transport into the three-dimensional EB structure.

EBs are used as a model system to study early embryonic development [11,14–17]. Of particular interest is the formation of a peripheral visceral endoderm (VE) layer during EB development [11,17]. BMP signaling within the EB is required for the formation of the VE layer [11,17]. This VE layer deposits a basement membrane, consisting of mainly collagen type IV and laminin, which provide sites for cell anchorage [11,17]. The basement membrane may also create a physical barrier to diffusive transport of inductive biochemicals.

EBs are also a useful system for generating large numbers of cells that may be needed for regenerative medicine. Scale-up of differentiated cells from EBs has been demonstrated [18,19] however the heterogeneity in differentiated cell types is a limitation to this method. This heterogeneity most likely arises due to internal concentration gradients of biochemicals within the EB. Concentration gradients have been shown to play a role in differentiation during embryonic development [20]. For example, gene expression of brachyury and goosecoid can be regulated by the concentration level of activin. Brachyury is activated when the concentration of activin is below a critical threshold whereas goosecoid becomes activated at concentrations above the threshold [20–22].

☆ *Editor's Note*: This paper is one of a newly instituted series of scientific articles that provide evidence-based scientific opinions on topical and important issues in biomaterials science. They have some features of an invited editorial but are based on scientific facts, and some features of a review paper, without attempting to be comprehensive. These papers have been commissioned by the Editor-in-Chief and reviewed for factual, scientific content by referees.

* Corresponding author. Tel.: +1 617 384 7980; fax: +1 617 495 9837.
E-mail address: auguste@seas.harvard.edu (D.T. Auguste).

0142-9612/$ – see front matter © 2008 Elsevier Ltd. All rights reserved.
doi:10.1016/j.biomaterials.2008.08.012

Understanding the underlying biological mechanisms that control diffusive transport and finding new ways to improve the effective exposure of inductive biochemicals during EB development may lead to more efficient differentiation strategies and more homogenous cell populations.

Several studies have reported techniques capable of producing EBs with uniform size in order to create a more homogenous environment [23–26]. However, these studies do not assess how concentration gradients change during EB development and do not identify the major obstacles to diffusive transport. We evaluate the role of diffusive transport during EB development by: 1) identifying key time points in EB development and characterizing the structural changes that influence diffusive transport dynamics; 2) defining the components of the EB shell; and 3) creating a strategy to increase diffusive transport by collagen inhibition or disruption of the shell. Finally, we demonstrate the importance of molecular diffusion by testing the impact of increased diffusive transport on the differentiation output of neuronal cells from EBs.

2. Materials and methods

2.1. EB culturing

Undifferentiated H9 hES cells were cultured on mitotically inactivated (via mitomycin C) mouse embryonic fibroblasts (MEFs) as previously described [27] (Supplementary Fig. 1). EBs were formed as previously described [28]. EBs were cultured in KO-DMEM supplemented with 20% FBS, 1% nonessential amino acids, 0.1 mM 2-mercaptoethanol, and 1 mM glutamine (denoted as EB media). Some EBs were cultured in EB media supplemented with 10^{-4} M azetidine carboxylic acid (AzC) (Sigma–Aldrich) or 100 ng/ml of human recombinant noggin (R&D Systems).

To facilitate diffusive transport, some EBs were treated for 15 min with 1 mg/ml collagenase B (Roche) (denoted as Ase in figures) at days 3, 4, 5, 6 and 7. After treatment, the collagenase was washed away and the EBs were cultured with fresh medium.

2.2. Scanning electron microscopy

For scanning electron microscopy analysis, EBs were fixed in 2.5% v/v glutaraldehyde in PBS before serial dehydration in ethanol and critical point dried with liquid CO_2. Samples were either Au or Pt–Pd coated and imaged with a SEM at an accelerating voltage of 2–3 kV. Same samples were sectioned with a razor blade to reveal internal EB features.

2.3. Immunofluorescence staining

Whole EBs were fixed with 2% w/v paraformaldehyde in PBS, blocked with 5% v/v normal goat serum and stained with mouse anti-human collagen IgG1 (1:250 dilution) (Sigma–Aldrich) followed by goat anti-mouse IgG1 conjugated to FITC (1:250 dilution) (Jackson ImmunoResearch) and Hoechst 33342 (Invitrogen) nuclear stain. Some samples were also stained with the cell membrane stain, 1,1′-dioctadecyl-3,3,3′,3′-tetramethylindodicarbocyanine perchlorate (DiD) (Invitrogen). The whole EBs were transferred onto glass slides and imaged using an epifluorescence microscope (Axiovert 200 M, Carl Zeiss).

EBs were also embedded in optimal cutting temperature (OCT) medium (Ted Pella) and frozen at −80 °C before being sectioned into 20 μm sections using a cryostat microtome. The sections were blocked with 5% normal goat serum (NGS) for 1 h, incubated with either monoclonal mouse anti-human collagen type IV (1:500 dilution) (Sigma Aldrich) or anti-human E-cadherin (1:250 dilution) (Chemicon) for 1 h followed by a 30 min incubation with goat anti-mouse IgG1 conjugated with FITC (1:250 dilution) (Jackson ImmunoResearch). Hoechst 33324 was used as a nuclear stain. Samples without primary antibody incubation acted as controls. Fluorescence images were taken using an epifluorescence microscope.

2.4. Diffusion profile

EBs were washed in PBS before being treated with 1 mg/ml solution of methylene blue (Sigma–Aldrich) in PBS for 10 min and then washed with PBS. EBs were embedded in OCT, frozen at −80 °C and sectioned with a cryostat microtome (20 μm thick slices). Digital images of the cross-sections were acquired using bright-field light microscopy and analyzed using ImageJ software (Supplementary Fig. 2). Color thresholds were defined to include only the blue dye component of the pixel data from which a grayscale radial profile was obtained. Some day 7 EBs were also exposed to 1 mg/ml collagenase B treatment for 15 min or 60 min before being prepared for radial diffusion profiling. Statistical analysis on EB shell intensity was conducted using a paired *t*-test. Cell viability of collagenase-treated EBs (Supplementary Fig. 3) was assessed using the Live/Dead assay (Invitrogen).

2.5. Neuronal differentiation

EBs were cultured in EB medium or EB medium supplemented with 10 μM all trans retinoic acid following the protocol described by Carpenter and co-workers [1]. EBs were divided into untreated (control group) and treated with daily collagenase digestions of 15 min on days 4, 5, 6 and 7 (treated group). Protein and gene expression were assessed on day 7 using flow cytometry or quantitative RT-PCR, respectively. For flow cytometry, the EBs were dissociated in to single cell suspensions by a 5 min trypsin incubation followed by 15 min incubation in non-enzymatic cell dissociation medium (Sigma–Aldrich) and stained for the neuronal surface marker, NCAM, using a rabbit polyclonal antibody (1:50 dilution) which was recognized with a goat anti-rabbit IgG secondary antibody conjugated to FITC at the same dilution. Samples stained with isotype antibodies acted as controls. Samples were analyzed with a flow cytometer (LSRII, BD Biosciences).

Quantitative RT-PCR was conducted by extraction of mRNA using the RNeasy Mini Kit (Qiagen) followed by conversion into cDNA (TaqMan Reverse Transcription Reagents, Applied Biosystems) and assessed by relative quantification with a real-time PCR (7300 Real-Time PCR System, Applied Biosystem) with the primers listed in Supplementary Table 1. Relative expression levels were calculated by the cycle threshold (Ct) relative quantification (RQ) method (ddCt,$RQ = 2^{-ddCt}$), using the cells cultured in EB medium and not treated with collagenase as the calibrator, and glyceraldehyde-3-phosphate dehydrogenase (GADPH) as the endogenous control. Each sample was tested in triplicate.

Some EBs were embedded in OCT, frozen and sectioned with a cryostat microtome. The sections were stained for collagen type IV and E-cadherin following the methods described in the immunostaining section.

3. Results

3.1. EB morphology, shell characterization and shell disruption

EBs undergo a transformation from a hES cell aggregate to a larger cystic body [28]. During this phase of structural changes, differentiation of hES cells into all 3 germ layers commences. We conducted a scanning electron microscopy survey over 14 days to observe morphological and topographical changes during EB formation, as summarized in Fig. 1. We find that day 1 EBs (Fig. 1A,B) undergo remodelling and synthesis of a fibrous ECM coating by day 3 (Fig. 1C,D). By day 7 (Fig. 1E,F), the voids between cells are filled with ECM resulting in a smoother surface topography. ECM deposition continues and by day 14 (Fig. 1G,H) the cell boundaries become indistinguishable. The EB surface begins as a multi-cellular cluster (days 1–3) with high surface area to volume (SA:V) ratio and is transformed to a smooth cell-matrix structure (day 7) with low SA:V ratio.

We proceeded to characterize the EB surface by determining the shell thickness and primary constituents. A cross-sectional view of a fractured day 7 EB (Fig. 2A) revealed a dense shell of approximately 20 μm thickness. The shell surrounds a cystic interior with cellular core components. The cellular network within the shell was observed by fluorescence staining of cell membranes using DiD and showed a squamous structure (Fig. 2B). We characterized the EB shell by immunofluorescence staining and found collagen type I to be a component of the surface (Fig. 2C,D taken at days 3 and 7, respectively). Stained cryostat cross-sections of EBs revealed the presence of collagen type IV lining the shell layer and internal cavities (Fig. 3A,B). E-cadherin was found to be present in the shell and throughout most of the EB as seen in Fig. 3C,D.

The observation that EBs formed a collagen type I coating of the surface and collagen type IV lining in the shell led us to investigate the impact of collagen formation on EB structure. We formed EBs in culture media supplemented with L-2-azetidine carboxylic acid (AzC), which is a known inhibitor of collagen synthesis [29–31]. The surface topography of EBs exposed to AzC for 7 days revealed pronounced cell boundaries (Fig. 4A,B) lacking the fibrous ECM seen in untreated EBs (compare Fig. 4A,B to Fig. 1E,F). Collagen type I was not detected on the surface of these EBs (Supplementary Fig. 4). However, collagen type IV was detected in the shell of EBs incubated with AzC as shown in Fig. 3E,F.

In comparison to AzC, noggin inhibits visceral endoderm and basement membrane formation [17]. Collagen type IV was sparsely

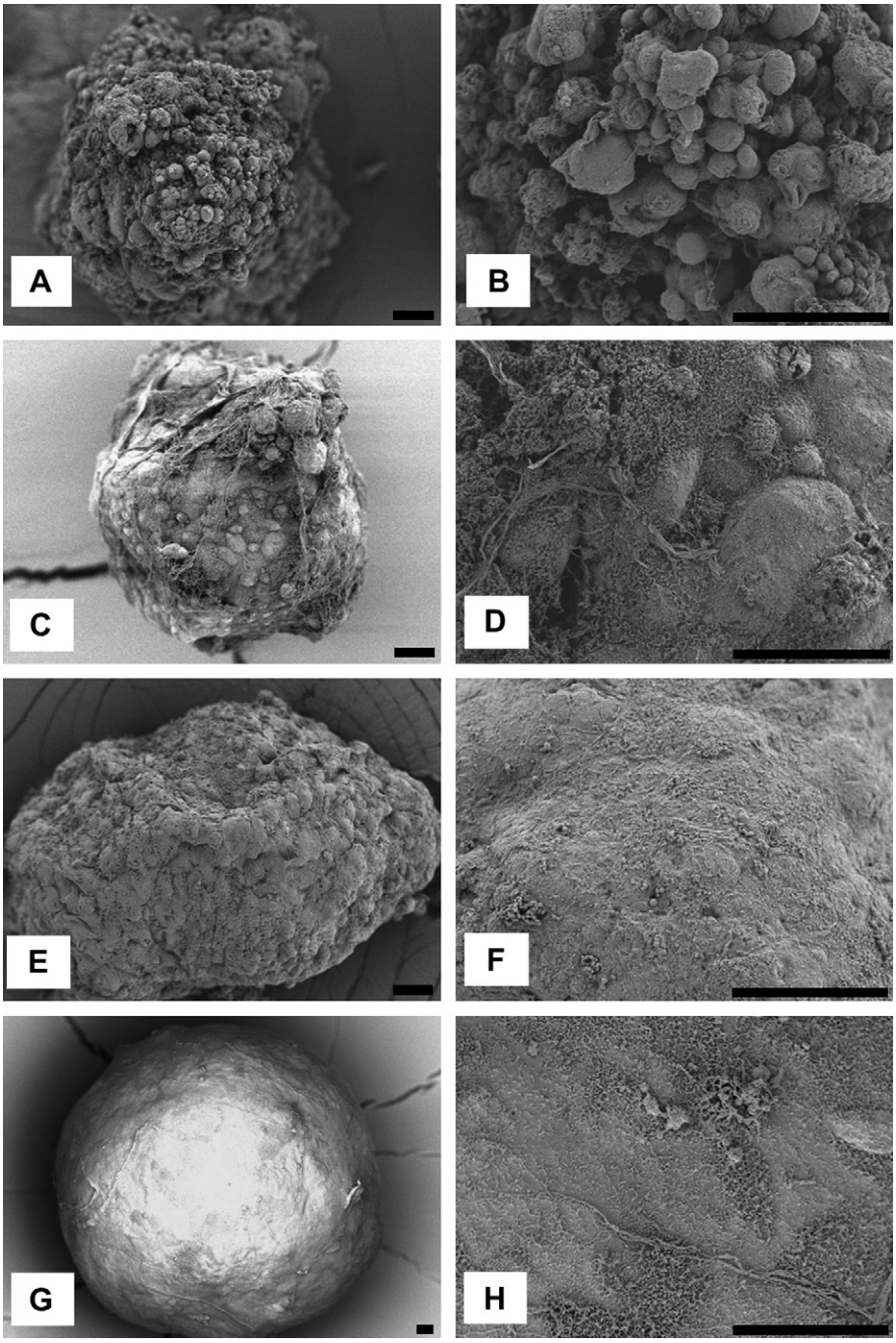

Fig. 1. Scanning electron micrographs of morphological (left column) and topographical changes (right column) in EB structure with culture time: (**A, B**) day 1 EB; (**C, D**) day 3 EB; (**E, F**) day 7 and (**G, H**) day 14 EB. EBs transform from dense lumpy cell clusters at days 1 and 3 to larger structures with a smoothened surface at days 7 and 14. The topography of a day 1 EB shows mostly cells but by day 3 a fibrous extracellular matrix network has developed. These cellular boundaries become interwoven with ECM by days 7 and 14. Scale bar, 20 μm.

found in EBs incubated with noggin (Fig. 3I,J) and was notably absent from the periphery of the EB. Scanning electron micrographs of noggin-incubated EBs revealed a surface structure similar to days 1 and 3 EBs (compare Fig. 4C,D to Fig. 1A–D) with pronounced cell boundaries.

As a consequence of the EBs having a collagen-rich shell, we investigated disrupting the shell with a mild enzymatic digestion. Collagenase B (collagenase) is a mixture of enzymes responsible for collagen degradation and is frequently used to dissociate hES cells from feeder layers or in breaking up EBs [8,14]. EBs treated with collagenase are denoted by "Ase" in the figures. EBs subjected to a daily 15 min collagenase digestion from day 4 onwards revealed the presence of collagen type IV and E-cadherin (Fig. 3M–P) similar to the pattern observed with untreated EBs (Fig. 3A–D). However, when assessed with scanning electron microscopy, it was found that collagenase treatment eroded the EB shell and created visible pores which revealed cell boundaries (compare Fig. 4E,F to Fig. 1F). Increasing the incubation time with collagenase does not appear to increase the pore size beyond 1 μm but does increase the number density of pores (an approximate threefold increase in pores after 60 min collagenase treatment relative to 15 min treatment). The morphology of digested day 7 EBs resembles that of days 1 and 3

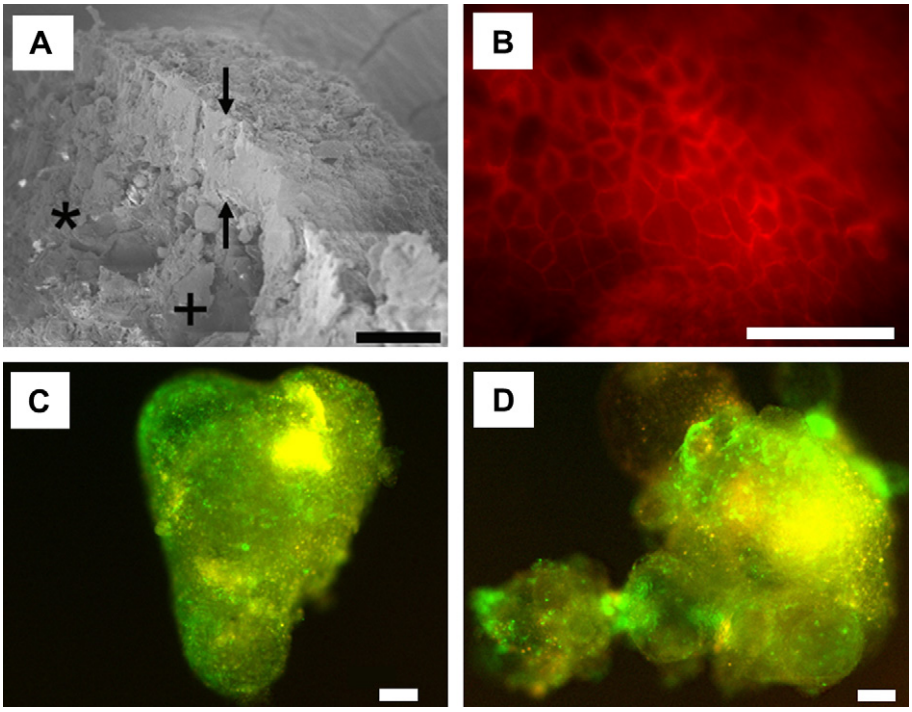

Fig. 2. Day 7 EB shell structure and characterization. (**A**) Fractured EB revealing the shell structure (arrows) and core (*) with void (+) components. (**B**) Cell membrane staining with DiD of day 14 EB showing the tight squamous cell-cell network that forms the shell. Immunofluorescence images of (**C**) day 3 EB, and (**D**) day 7 EB. EBs stained with monoclonal mouse anti-collagen conjugated to FITC (green) and merged with autofluorescence emission under a Texas Red filter. Due to high levels of broad spectrum autofluorescence observed in EBs, the yellow is attributed to autofluorescence whereas the green shows positive staining of collagen on the shell. Scale bar, 20 μm (**A**); 100 μm (**B–D**).

EBs with regards to exposed cell boundaries (compare Fig. 3E,F to Fig. 1B,D). Creation of pores by collagen digestion may allow penetration of inductive biochemicals (and other media components) within the EB, facilitating a more homogenous exposure to throughout the shell.

3.2. EB diffusive transport

In order to assess the impact of EB shell formation on the diffusive transport of exogenous biochemicals, we developed a semi-quantitative methylene blue (Mb) diffusion assay. Mb has been broadly used in assessing diffusion in biological systems [32]. We considered the effect of EB age and changes due to treatment with AzC, noggin and collagenase on molecular diffusion into the EB. On day 3, Mb radially diffuses into the EB and is taken up in high concentrations by the outermost cells (Fig. 5A). As EBs remodel and proceed to become cystic (Fig. 5B), we note a reduction in Mb uptake within the EB shell layer (Fig. 5B,C).

From cryosectioned samples (Fig. 5A–C) we quantified the ability of Mb to penetrate EBs of (1) different age (Fig. 5D); (2) with their ECM disrupted by AzC and noggin (Fig. 5E); and (3) disrupted with collagenase for 15 min or 60 min (Fig. 5E). One consequence of comparing EBs of different ages (Fig. 5D) is that the radius increases with time as is evident in the graphs. We observe high uptake of Mb on day 3 throughout the EB, but by day 7, when EBs have become cystic, Mb uptake within the shell has significantly decreased by greater than 80% relative to day 3 (Fig. 5F) and remains at this level until the end of the study at day 14. EBs treated with AzC had similar Mb diffusion profiles as untreated EBs at day 7 (Fig. 5F). Incubation with noggin however increased the uptake of Mb within 68% of the level observed with day 3 EBs. Treatment with collagenase also improved diffusion of Mb within the EB by 25% and approximately 40% for 15 min and 60 min digestions, respectively. The peak intensity of the shell for each treatment (Fig. 5F) confirmed that a significant improvement of Mb transport by diffusion is obtained after incubation with noggin and collagenase for 15 min or 60 min relative to untreated day 7 EBs.

3.3. Neuronal differentiation

We hypothesized that increased diffusive transport of RA by collagenase treatment may facilitate the differentiation of hES cells into neuronal cells. Immunofluorescence stained sections of EBs incubated with RA showed similar features to EBs cultured in EB medium with respect to collagen type IV immunoreactivity (compare Fig. 6A–D to Fig. 3A–D). This collagen is present mostly near the shell layer. However, the EBs treated with RA differed in that they had markedly reduced cysts and higher expression of E-cadherin at the periphery. Treating the RA supplemented EBs with collagenase appears to decrease collagen type IV along the shell, although it is still detectable in the EB (Fig. 6E,F). The expression of E-cadherin in collagenase treated EBs (Fig. 6G,H) is not altered relative to untreated EBs or EBs incubated with RA.

Flow cytometric analysis of NCAM expression showed that day 7 EBs treated with daily collagenase digestions with or without RA supplementation had a greater population of NCAM positive cells relative to untreated EBs (Fig. 7A,B). In the absence of RA (Fig. 7A) and without collagenase treatment, 32% of cells in the EBs differentiate into NCAM expressing cells. This population increases by approximately 67% when the EBs were treated with collagenase to permeabilize the shell. A similar comparison is found when comparing EBs with and without collagenase treatment and cultured in the presence of RA (Fig. 7B). EBs supplemented with RA but not treated with collagenase had approximately 28% of cells expressing NCAM. This population increased to 68% when treated with collagenase and cultured with RA. This trend was further confirmed by quantitative RT-PCR which revealed increased NCAM expression in treated EBs (with and without RA supplementation)

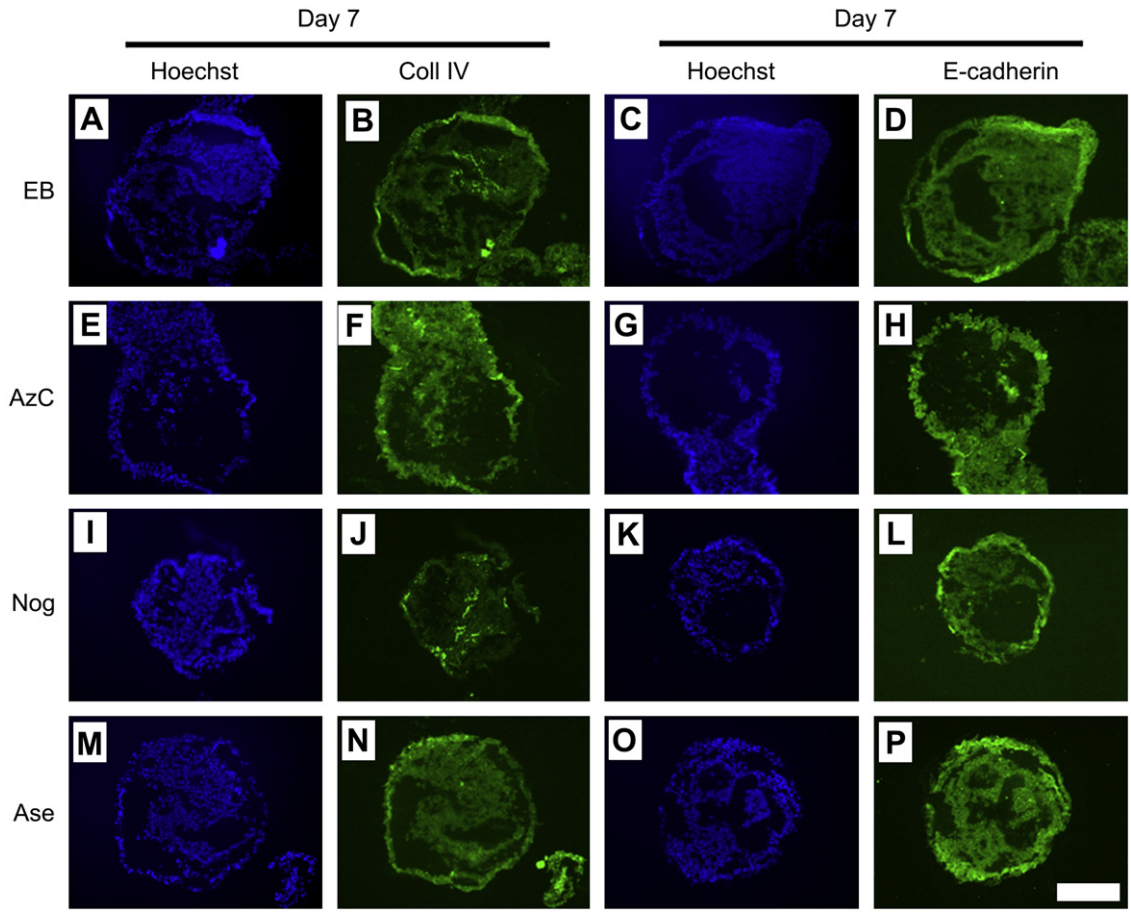

Fig. 3. Immunofluorescence staining of cryostat sectioned day 7 EBs (**A–D**) **EB**, incubated in EB medium; (**E–H**) **AzC**, supplemented with AzC; (**I–L**) **Nog**, supplemented with noggin; and (**M–P**) **Ase**, treated daily with collagenase for 15 min from days 4–7. (**B, F, J, N**) Collagen type IV staining and (**D, H, L, P**) E-cadherin is shown alongside nuclear staining (**A, E, I, M**) and (**C, G, K, O**), respectively. Collagen type IV is found in EBs incubated in EB medium, AzC and treated with collagenase. There is a marked reduction in collagen type IV and cyst formation in EBs incubated with noggin. E-cadherin is expressed throughout EBs incubated with EB medium, AzC and treated with collagenase. Scale bar, 200 μm.

and untreated EBs supplemented with RA relative to untreated EBs (Fig. 7C). The largest increase in NCAM expression was observed in EBs cultured with RA and treated with collagenase followed by EBs without RA supplementation but treated with collagenase and then EBs supplemented with RA.

4. Discussion

Early EB development involves the transformation from a cellular aggregate to a cystic body (Fig. 1). Structural contributions from cell–cell adhesions and ECM deposition are most likely involved in this transformation process. The activation of E-cadherin (Fig. 3) has been shown to be critical in the formation of cell–cell adhesions within the EB [18] creating a squamous cell surface (Fig. 2B). Our investigation however focuses on the role of ECM development within the EB and its impact on molecular diffusion.

As EBs develop, paracrine and autocrine signaling contribute to directing stem cell fate. This signaling may create concentration gradients within the EB which can influence EB transformation and differentiation. Inductive biochemicals, which have been solubilized in the media, are used to maintain or alter these internal concentration gradients to favor differentiation of a specific lineage. We show that transformation of the EB, and in particular the contribution from the ECM deposition, has a defining role in molecular diffusion of biochemicals which regulates stem cells differentiation.

During EB development, a fibrous ECM is secreted on the EB surface from day 3 and continues to form until the surface is completely coated (Fig. 1). Immunofluorescence staining of the EB surface confirmed that collagen type I is a constituent of this ECM coating (Fig. 2B). Collagen type IV was detected in the outer most cell layer and lining of internal cavities (Fig. 3B). Formation of this collagen type I coating can be inhibited by culturing the EB in the presence of AzC (Supplementary Fig. 4 and Fig. 4A,B). This chemical inhibits collagen synthesis by acting as a proline analogue and interfering with the formation of the collagen triple-helix [33]. This hinders tropocollagen formation and self-assembly into fibers. AzC incubation did not inhibit collagen type IV formation (Fig. 3F). The mode of AzC action as a proline analogue may inhibit collagen type IV synthesis less than type I fiber formation. This may be due to the differences in protein structure between the two collagen types. Collagen type IV creates a sheet-like structure instead of fibers. Although collagen type IV does possess a triple-helix section, it also has hydroxyproline-free, globular non-collagenous (NC) domains [34]. Two collagen type IV molecules bind NC-to-NC domains. This binding may allow for stabilization of collagen type IV and self-assembly of the basement membrane. In contrast, collagen type I forms fibers by parallel self-assembly of tropocollagen molecules in a quarter-staggered array structure which is dependent on intermolecular crosslinks to stabilize the fiber [35]. AzC appears to be selective in inhibiting collagen type I deposition on the surface but not collagen type IV, a major component of the basement membrane.

Collagen type IV was instead disrupted by inhibiting the formation of the visceral endoderm (VE) peripheral cell layer that develops in EBs [17]. This VE layer, which creates the basement

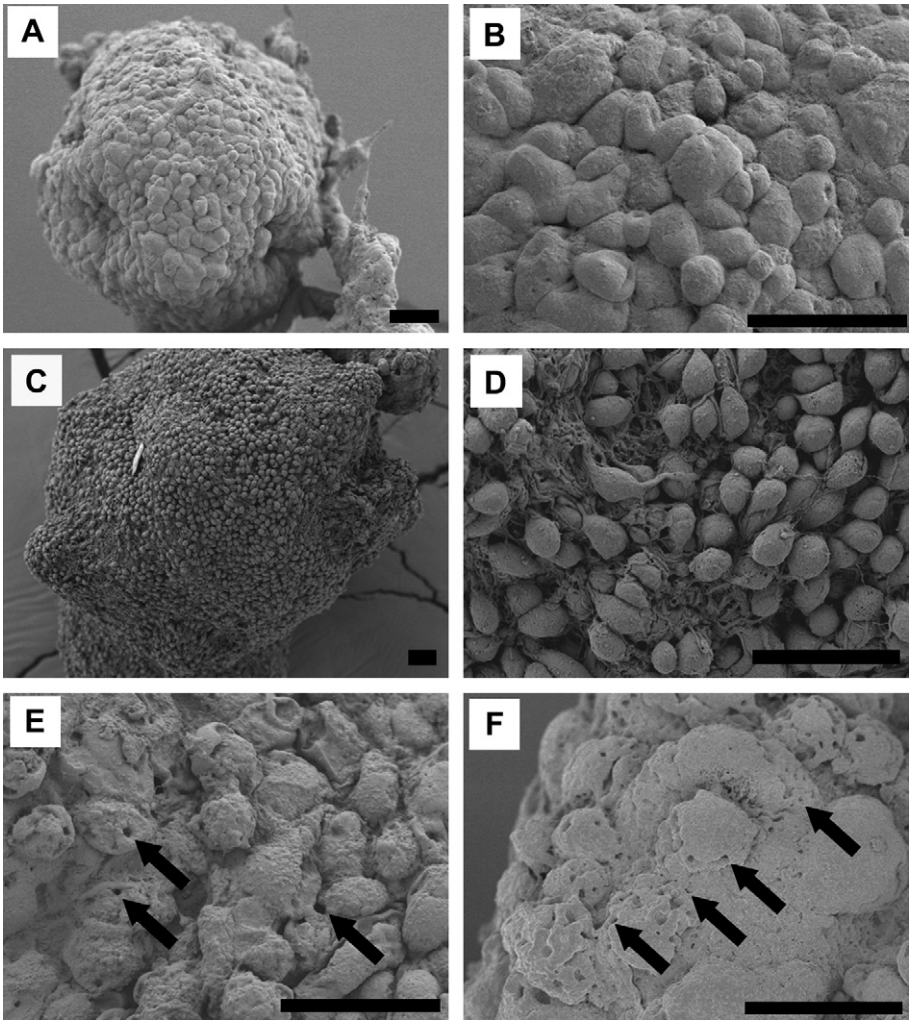

Fig. 4. SEM micrographs showing the shell of day 7 EB after treatment with: (**A, B**) azetidine carboxylic acid; (**C, D**), noggin; (**E**) collagenase B treatment for 15 min; and (**F**) collagenase treatment for 60 min. EBs treated with AzC possess a surface with well defined cell boundaries that lacks the ECM coating noted in Fig. 1F. Incubation with noggin created EBs which lack cellular cohesiveness and the ECM coating. EBs treated with collagenase B for (**E**) 15 min and (**F**) 60 min developed pores (arrows) on the surface of the shell as well as exposing cell boundaries. Scale bar, 20 μm.

membrane [11,17], can be inhibited by incubating the EBs with noggin. Noggin is a BMP antagonist which also reduces cavity formation [17]. As a consequence of noggin inhibition, collagen type IV found in the basement membrane is not deposited (Fig. 3J). SEM micrographs of EBs cultured with noggin for 7 days revealed a surface topography similar to that of days 1 and 3 EBs with well-defined cell boundaries.

We conclude that the EB shell is a trilayer structure consisting of 1) a superficial outer ECM layer of which collagen type I is a predominant component; 2) a squamous cell layer; and 3) an underlying basement membrane. Diffusive transport of a soluble biochemical into an EB depends on its ability to penetrate this shell.

We find that formation of a 20 μm shell after EB development for 7 days reduces diffusive transport of Mb into the EB (Fig. 5). We interpret the measured decrease in Mb uptake as evidence of a reduction in diffusive transport across the shell layer. Reduced diffusive transport may be more pronounced for large molecular weight growth factors (the molecular weight of bFGF is 17 kDa and Mb is 0.374 kDa), which raises the question as to the efficiency of current EB culture strategies using soluble biochemicals to induce differentiation.

We assessed three different methods to increase diffusive transport by disrupting the shell using: 1) incubation with AzC to inhibit the formation of collagen type I; 2) incubation with noggin to inhibit basement membrane formation; and 3) treatment with collagenase to penetrate the shell. We find that inhibition of collagen type I by AzC does not increase diffusive transport, whereas inhibition of collagen type IV from the basement membrane restores the diffusive transport to levels comparable to that of day 3 EBs. This leads us to identify the basement membrane as the major obstacle to diffusive transport in EBs.

We hypothesized that increased diffusive transport of an inductive biochemical would promote the differentiation of cells within the EB. Although noggin treatment resulted in the highest diffusive transport of day 7 EBs, its antagonist actions in BMP signaling and documented affects on differentiation [36] create an uncontrollable variable for testing our hypothesis. For this reason, we decided to use a 15-min collagenase digestion to structurally permeabilize the basement membrane and increase diffusive transport in the EB. Collagenase treatment may initiate other events that have yet to be identified, but our immunostaining showed that treated EBs retained similar structural features with regards to collagen type IV deposition and expression of E-cadherin.

We have shown that enzymatic digestion using collagenase creates pores in the EB shell which facilitates diffusive transport. This treatment degrades the outer ECM's collagen type I and the basement membrane's collagen type IV, making the EBs more

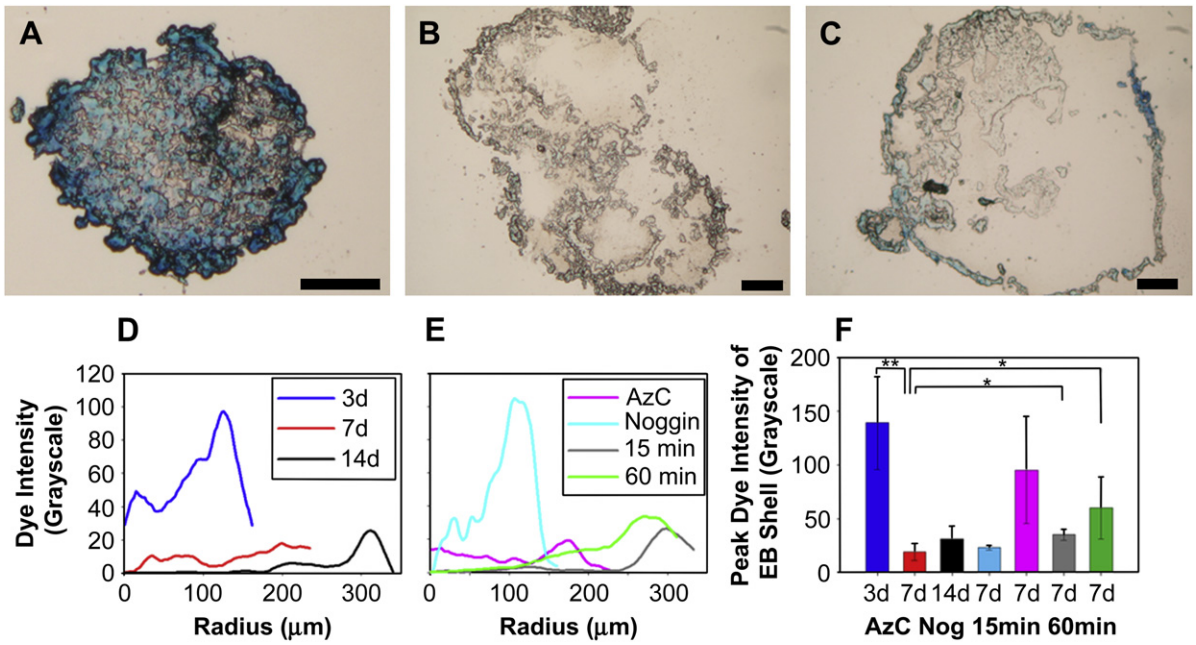

Fig. 5. Methylene blue uptake radial diffusion profiles of EBs. Bright-field images of sectioned (**A**) day 3, (**B**) day 7 and (**C**) day 14 EBs after exposure to methylene blue. (**D**) Radial diffusion profiles of EBs over culture time. (**E**) Radial profile of EB treated with AzC, noggin and collagenase B treatment for 15 min (15 min) or 60 min (60 min). (**F**) Peak dye intensity of EB shell for the different groups. Mean values ± s.d. are shown. A significant difference in intensity is found between day 3 versus day 7 EBs ($^{**}p < 0.01$) and day 7 EBs versus collagenase B treated EBs ($^{*}p < 0.05$, $n = 3$ per group). Scale bar, 200 μm.

permeable to soluble biochemicals. Collagenase intervention can therefore be used as a method to increase the diffusive transport of biochemicals into the EB post-shell formation.

In order to assess whether increased diffusive transport contributes to neuronal cell differentiation, we added RA to EBs treated with a daily 15 min collagenase digestion after shell formation on day 4. RA is a biochemical reported to promote differentiation of neuronal cells from hES cells and has a molecular weight (300 Da) comparable to Mb. We find that collagenase treatment is able to increase the expression of NCAM positive cells irrespective of whether RA is present in the medium relative to untreated EBs. The increase in NCAM expression by flow cytometry and qRT-PCR is indicative of a higher output of neuronal differentiation due to increased diffusive transport of RA and serum. The highest NCAM expression was detected in EBs treated with collagenase and supplemented RA followed by EBs treated with collagenase and then untreated EBs supplemented with RA. This trend reasserts the increased output of neuronal cells following permeabilization of EBs. Higher NCAM expression may occur due to increased diffusive transport which occurs after shell modification.

Numerous studies have shown the inductive properties of soluble biochemicals on EBs grown for more than 4 days [1,6–8,10,14]. Our findings suggest that the induction most probably occurs before the formation of a shell, which in EBs from H9 hES cells occurs between days 3 and 7. The transitory nature of the EB shell can also explain the heterogeneity of differentiated cell populations derived from EBs. Reduced diffusive transport would result in altered concentration gradients of inductive soluble

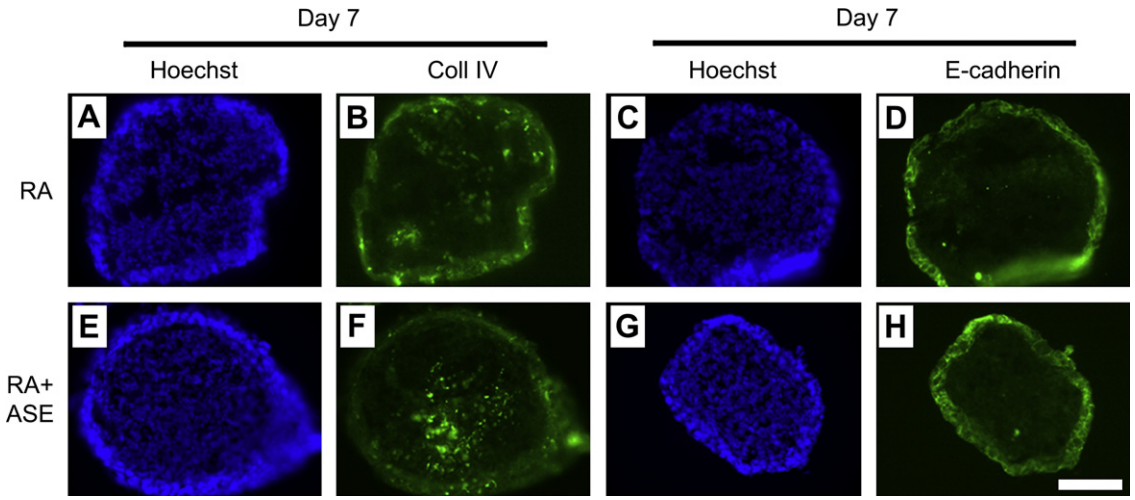

Fig. 6. Immunofluorescence staining of cryosectioned EBs (**A–D**) supplemented with retinoic acid (**RA**) for 7 days; and (**E–H**) supplemented with RA and treated daily with collagenase for 15 min from days 4–7 (**RA** + **Ase**). (**B, F**) Collagen type IV and (**D, H**) E-cadherin staining is shown alongside nuclear staining (**A, E**) and (**C, G**), respectively. Collagen type IV is found lining the outer periphery of EBs supplemented with RA. Collagenase treatment appears to reduce this lining. E-cadherin is localized to the outer periphery of both untreated and treated EBs. Scale bar, 100 μm.

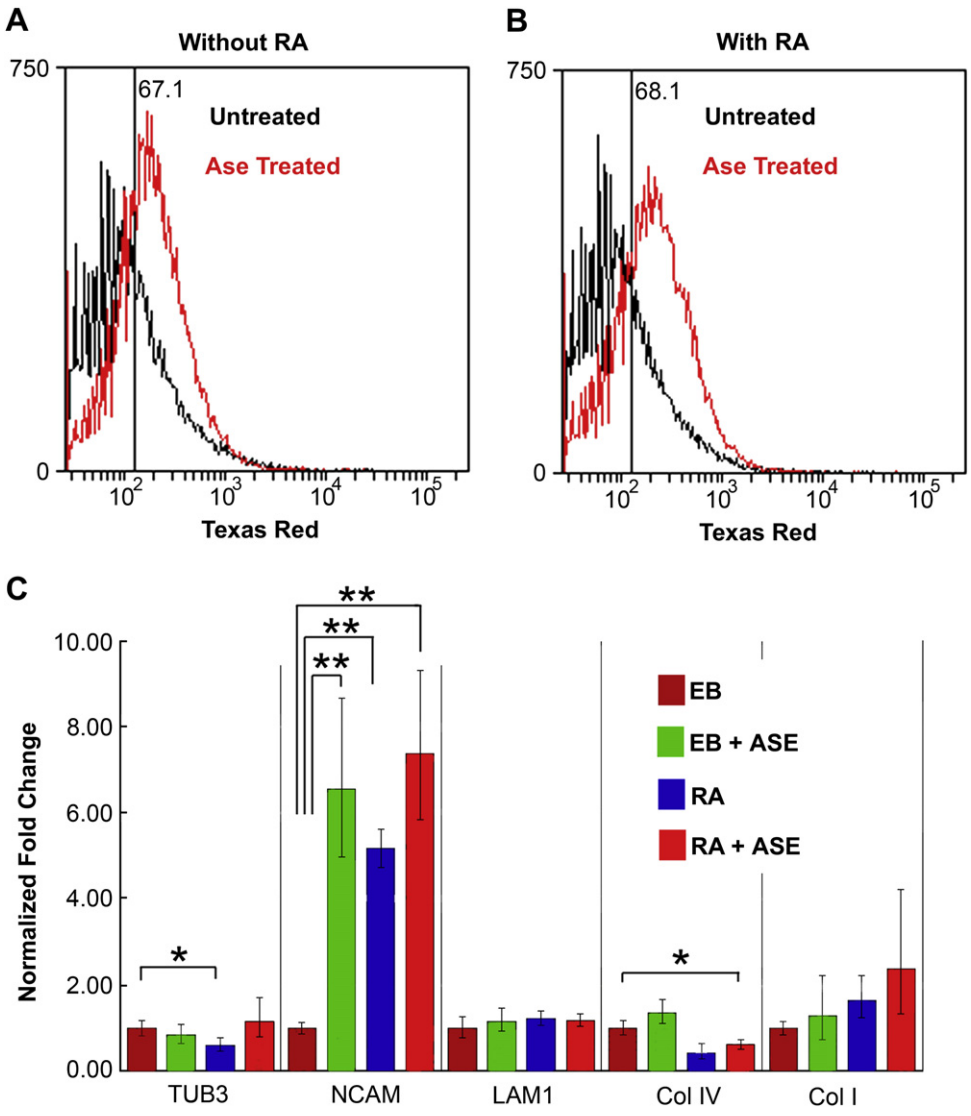

Fig. 7. Differentiation output of EBs. (A–B) Flow cytometry of NCAM stained cells. EBs treated with daily collagenase digestion for 15 min from days 4–7 (**Ase treated**) showed a higher intensity of NCAM expression relative control EBs (**untreated**) when incubated with or without RA. (**C**) Quantitative RT-PCR of EBs under the same conditions. EBs cultured in EB medium (**EB**) and treated with collagenase (**EB + Ase**) were compared to EBs cultured in medium supplemented with RA (**RA**) and treated with collagenase (**RA + Ase**). A significant increase in NCAM expression is observed for EBs treated with collagenase (with and without RA supplementation) relative to untreated EBs incubated without RA supplementation. To a lesser degree, untreated EBs incubated with RA also showed a significant increase in NCAM expression ($^{*}p < 0.05$, $^{**}p < 0.01$, $n = 3$ per group)

biochemicals which may activate different genes, similar to how activin induces activation of brachyury and goosecoid when its concentration is below or above a critical threshold, respectively [20–22]. Controlled EB exposure to inductive biochemicals at levels below or above critical thresholds may lead to an increased output of differentiated cells and a more homogenous population. A more uniform concentration gradient during culture of EBs may assist in cell lineage expansion for cell therapies.

During normal embryo development, the generation of tissue-specific cell types is likely to arise from both physical (three-dimensional cell–cell adhesions) and biochemical (morphogen-mediated) signals. EBs recapitulate some of these physical and biochemical signals. We have attempted to understand how biochemical signaling and physical three-dimensional cues may facilitate differentiation. We show that within our system, increased diffusive transport of an inductive biochemical can lead to increased differentiation of stem cells.

A reduction in diffusive transport of serum components may be responsible for initiating several key events in EB development. For example, it has been shown that the activation of mitochondrial apoptosis-inducing factor (AIF) results in the programmed cell death of core cells in the EB leading to the formation of a cystic body [37]. Serum deprivation triggers apoptosis of embryonic stem cells whereas genetically inactivated AIF embryonic stem cells were resistant to cell death under the same conditions. Our findings suggest that EB shell formation, which reduces diffusive transport, is similar to depriving the core cells of serum which may lead to the activation of AIF and initiation of morphogenetic changes. Similar outcomes may be expected due to hypoxia arising from reduced diffusive transport and activation of hypoxia inducible factor (HIF) which can lead to apoptosis [38] as well as activation of vasculogenesis [39].

Furthermore, oxygen deprivation may trigger the differentiation of stem cells into progenitor cells of the circulatory system. Hemangioblast cells arise in EBs within 3–4 days of differentiation [14]. When taken in context with the findings reported here, EB shell formation coincides with the development of hematopoietic and vascular systems. Serum-free conditions, which simulate zero diffusion, have also been shown to increase differentiation into cardiomyocytes [40].

The relationship between biochemical molecular weight and diffusive transport in EBs still remains to be elucidated. In addition, the impact of shell disruption on differentiation requires further investigation. We suspect a biophysical mechanism involving diffusive transport of exogenous biochemicals may play a key role in EB formation and embryogenesis.

5. Conclusions

In this paper, we have shown that control over molecular transport plays a strategic role in stem cell differentiation. During the first few days of development, ECM proteins are deposited on the EB exterior, comprising a trilayer shell structure. This shell consists of 1) a superficial outer ECM layer of which collagen type I is a predominant component; 2) a squamous cell layer bound by E-cadherin; and 3) an underlying basement membrane (primarily made of collagen type IV and laminin). The basement membrane is identified as the major barrier to diffusive transport from day 3 onwards.

We hypothesized that control over molecular transport could be exploited to impact hES cell differentiation. Permeabilizing the EB shell was achieved by an enzymatic digestion using collagenase, which results in pores in the EB shell. Collagenase-treated EBs had a higher expression of NCAM positive cells relative to untreated EBs. This is due to the increase in molecular diffusion of retinoic acid and other serum components into EBs, thereby promoting differentiation into NCAM expressing cells.

Our results suggest that diffusive transport of inductive biochemicals in EBs should be considered when formulating differentiation protocols. Consequently, diffusive transport in EBs can be manipulated to facilitate differentiation.

Acknowledgements

This work was supported by Harvard MRSEC (no. DMR-0213805). We thank H.A. Stone, D. Mooney and R. Nagpal for critical reading of the manuscript. C. Mummery is thanked for her thoughtful suggestions and feedback. We thank A.Vahdatshoar and A. Singh Grawal for technical assistance. We declare no conflict of interest.

Appendix. Supplementary material

Supplementary data associated with this article can be found, in the online version, at doi:10.1016/j.biomaterials.2008.08.012

References

[1] Carpenter MK, Inokuma MS, Denham J, Mujtaba T, Chiu CP, Rao MS. Enrichment of neurons and neural precursors from human embryonic stem cells. Exp Neurol 2001;172(2):383–97.
[2] Wobus AM, Guan KM, Jin S, Wellner MC, Rohwedel J, Ji GJ, et al. Retinoic acid accelerates embryonic stem cell-derived cardiac differentiation and enhances development of ventricular cardiomyocytes. J Mol Cell Cardiol 1997;29(6):1525–39.
[3] Schuldiner M, Eiges R, Eden A, Yanuka O, Itskovitz-Eldor J, Goldstein RS, et al. Induced neuronal differentiation of human embryonic stem cells. Brain Res 2001;913(2):201–5.
[4] Takahashi T, Lord B, Schulze PC, Fryer RM, Sarang SS, Gullans SR, et al. Ascorbic acid enhances differentiation of embryonic stem cells into cardiac myocytes. Circulation 2003;107(14):1912–6.
[5] Shin DM, Ahn JI, Lee KH, Lee YS, Lee YS. Ascorbic acid responsive genes during neuronal differentiation of embryonic stem cells. Neuroreport 2004;15(12):1959–63.
[6] Kehat I, Kenyagin-Karsenti D, Snir M, Segev H, Amit M, Gepstein A, et al. Human embryonic stem cells can differentiate into myocytes with structural and functional properties of cardiomyocytes. J Clin Invest 2001;108(3):407–14.
[7] Dani C, Smith AG, Dessolin S, Leroy P, Staccini L, Villageois P, et al. Differentiation of embryonic stem cells into adipocytes in vitro. J Cell Sci 1997;110:1279–85.
[8] Chadwick K, Wang LS, Li L, Menendez P, Murdoch B, Rouleau A, et al. Cytokines and BMP-4 promote hematopoietic differentiation of human embryonic stem cells. Blood 2003;102(3):906–15.
[9] Wiles MV, Keller G. Multiple hematopoietic lineages develop from embryonic stem (Es) cells in culture. Development 1991;111(2):259.
[10] Kramer J, Hegert C, Guan KM, Wobus AM, Muller PK, Rohwedel J. Embryonic stem cell-derived chondrogenic differentiation in vitro: activation by BMP-2 and BMP-4. Mech Dev 2000;92(2):193–205.
[11] Coucouvanis E, Martin GR. BMP signaling plays a role in visceral endoderm differentiation and cavitation in the early mouse embryo. Development 1999;126(3):535–46.
[12] Vittet D, Prandini MH, Berthier R, Schweitzer A, MartinSisteron H, Uzan G, et al. Embryonic stem cells differentiate in vitro to endothelial cells through successive maturation steps. Blood 1996;88(9):3424–31.
[13] Kubo A, Shinozaki K, Shannon JM, Kouskoff V, Kennedy M, Woo S, et al. Development of definitive endoderm from embryonic stem cells in culture. Development 2004;131(7):1651–62.
[14] Kennedy M, D'Souza SL, Lynch-Kattman M, Schwantz S, Keller G. Development of the hemangioblast defines the onset of hematopoiesis in human ES cell differentiation cultures. Blood 2007;109(7):2679–87.
[15] Vallier L, Pedersen RA. Human embryonic stem cells – an in vitro model to study mechanisms controlling pluripotency in early mammalian development. Stem Cell Rev 2005;1(2):119–30.
[16] Dvash T, Sharon N, Yanuka O, Benvenisty N. Molecular analysis of LEFTY-expressing cells in early human embryoid bodies. Stem Cells 2007;25(2):465–72.
[17] Conley BJ, Ellis S, Gulluyan L, Mollard R. BMPs regulate differentiation of a putative visceral endoderm layer within human embryonic stem-cell-derived embryoid bodies. Biochem Cell Biol 2007;85(1):121–32.
[18] Fok EYL, Zandstra PW. Shear-controlled single-step mouse embryonic stem cell expansion and embryoid body-based differentiation. Stem Cells 2005;23(9):1333–42.
[19] Gerecht-Nir S, Cohen S, Itskovitz-Eldor J. Bioreactor cultivation enhances the efficiency of human embryoid body (hEB) formation and differentiation. Biotechnol Bioeng 2004;86(5):493–502.
[20] Gurdon JB, Harger P, Mitchell A, Lemaire P. Activin signaling and response to a morphogen gradient. Nature 1994;371(6497):487–92.
[21] Gurdon JB, Mitchell A, Mahony D. Direct and continuous assessment by cells of their position in a morphogen gradient. Nature 1995;376(6540):520–1.
[22] McDowell N, Zorn AM, Crease DJ, Gurdon JB. Activin has direct long-range signalling activity and can form a concentration gradient by diffusion. Curr Biol 1997;7(9):671–81.
[23] Ungrin MD, Joshi C, Nica A, Bauwens C, Zandstra PW. Reproducible, ultra high-throughput formation of multicellular organization from single cell suspension-derived human embryonic stem cell aggregates. PLoS ONE 2008;3(2):e1565.
[24] Carpenedo RL, Sargent CY, McDevitt TC. Rotary suspension culture enhances the efficiency, yield, and homogeneity of embryoid body differentiation. Stem Cells 2007;25(9):2224–34.
[25] Park J, Cho CH, Parashurama N, Li YW, Berthiaume F, Toner M, et al. Microfabrication-based modulation of embryonic stem cell differentiation. Lab Chip 2007;7(8):1018–28.
[26] Torisawa YS, Chueh BH, Huh D, Ramamurthy P, Roth TM, Barald KF, et al. Efficient formation of uniform-sized embryoid bodies using a compartmentalized microchannel device. Lab Chip 2007;7(6):770–6.
[27] Thomson JA, Itskovitz-Eldor J, Shapiro SS, Waknitz MA, Swiergiel JJ, Marshall VS, et al. Embryonic stem cell lines derived from human blastocysts. Science 1998;282(5391):1145–7.
[28] Itskovitz-Eldor J, Schuldiner M, Karsenti D, Eden A, Yanuka O, Amit M, et al. Differentiation of human embryonic stem cells into embryoid bodies comprising the three embryonic germ layers. Mol Med 2000;6(2):88–95.
[29] Takeuchi T, Prockop DJ. Biosynthesis of abnormal collagens with amino acid analogues.I. Incorporation of L-azetidine-2-carboxylic acid and cis-4-fluoro-L-proline into protocollagen and collagen. Biochim Biophys Acta 1969;175(1):142.
[30] Lane JM, Dehm P, Prockop DJ. Effect of proline analogue azetidine-2-carboxylic acid on collagen synthesis in-vivo .1. Arrest of collagen accumulation in growing chick embryos. Biochim Biophys Acta 1971;236(3):517.
[31] Sato H, Takahashi M, Ise H, Yamada A, Hirose S, Tagawa Y, et al. Collagen synthesis is required for ascorbic acid-enhanced differentiation of mouse embryonic stem cells into cardiomyocytes. Biochem Biophys Res Commun 2006;342(1):107–12.
[32] Vignaud JM, Menard O, Weinbreck N, Siat J, Borrelly J, Marie B, et al. Evaluation of the spatial diffusion of methylene blue injected in vivo by bronchoscopy into non-small cell lung carcinoma. Respiration 2006;73(5):658–63.
[33] Zagari A, Palmer KA, Gibson KD, Nemethy G, Scheraga HA. The effect of the L-azetidine-2-carboxylic acid residue on protein conformation.4. Local substitutions in the collagen triple-helix. Biopolymers 1994;34(1):51–60.
[34] LeBleu VS, MacDonald B, Kalluri R. Structure and function of basement membranes. Exp Biol Med 2007;232(9):1121–7.
[35] Kadler KE, Holmes DF, Trotter JA, Chapman JA. Collagen fibril formation. Biochem J 1996;316:1–11.
[36] Pera MF, Andrade J, Houssami S, Reubinoff B, Trounson A, Stanley EG, et al. Regulation of human embryonic stem cell differentiation by BMP-2 and its antagonist noggin. J Cell Sci 2004;117(7):1269–80.

[37] Joza N, Susin SA, Daugas E, Stanford WL, Cho SK, Li CYJ, et al. Essential role of the mitochondrial apoptosis-inducing factor in programmed cell death. Nature 2001;410(6828):549–54.
[38] Carmeliet P, Dor Y, Herbert JM, Fukumura D, Brusselmans K, Dewerchin M, et al. Role of HIF-1 alpha in hypoxia-mediated apoptosis, cell proliferation and tumour angiogenesis [vol. 394, p. 485, 1998]. Nature 1998;395(6701):525.
[39] Ramirez-Bergeron DL, Runge A, Adelman DM, Gohil M, Simon MC. HIF-dependent hematopoietic factors regulate the development of the embryonic vasculature. Dev Cell 2006;11(1):81–92.
[40] Passier R, Oostwaard DWV, Snapper J, Kloots J, Hassink RJ, Kuijk E, et al. Increased cardiomyocyte differentiation from human embryonic stem cells in serum-free cultures. Stem Cells 2005;23(6):772–80.